Catal Surv Asia (2008) 12:188–202
DOI 10.1007/s10563-008-9051-7

Hydrogen Production by Catalytic Reforming of Gaseous Hydrocarbons (Methane & LPG)

Dong Ju Moon

Abstract Hydrogen has been attracting great interest as a major energy source in near future. The lack of an infrastructure has led to a research effort to develop fuel processing technology for production of hydrogen. In this review, we are reporting the catalytic reforming of gaseous hydrocarbons carried out in our research group, covering dry-reforming of CH_4, tri-reforming of CH_4, the electrocatalytic reforming of CH_4 by CO_2 in the SOFC (solid oxide fuel cell) system and steam reforming of LPG. Especially, we have focused on our work, though the related work from other researchers is also discussed wherever necessary. It was found that tri-reforming of CH_4 over NiO–YSZ–CeO_2 catalyst was more desirable than dry-reforming of CH_4 due to higher reforming activity and less carbon formation. The synthesis gas produced by tri-reforming of CH_4 can be used for the production of dimethyl ether, Fischer–Tropsch synthesis fuels and high valued chemicals. To improve the problem of deactivation of catalyst due to carbon formation in the dry reforming of CH_4, the internal reforming of CH_4 by CO_2 in SOFC system with NiO–YSZ–CeO_2 anode catalyst was suggested for cogeneration of a syngas and electricity. It was found that Rh-*spc*-Ni/MgAl catalyst showed long term stability for 1,100 h in the steam reforming of LPG under the tested conditions. The addition of Rh to *spc*-Ni/MgAl catalyst restricted the deactivation of catalyst due to carbon formation in the steam reforming of LPG and diesel under the tested conditions. The result suggested that the developed reforming catalysts can be used in the reforming process of CH_4, LNG and LPG for application to hydrogen station and fuel processor system.

Keywords Catalytic reforming · Hydrogen production · Fuel-cell powered vehicles · Fuel processor system · Hydrogen station · SOFC · Internal reforming · PEM fuel cell · Dry-reforming · Tri-reforming · Steam reforming · CH_4 · LPG

1 Introduction

Hydrogen is forecast to become a major source of energy in near future. Molecular hydrogen is an ecofriendly fuel which can be converted to electricity efficiently via fuel cells with zero emissions of greenhouse gases or hazardous species such as volatile organic compounds [1–5].

Hydrogen has been used in a number of industrial applications, like ammonia production, oil refineries and methanol production plants. Most of the hydrogen has been produced as an industrial scale by the process of steam reforming of natural gas or as a byproduct of petroleum refining and chemicals production. Generally, hydrogen can be produced by the following processes such as steam reforming (SR), partial oxidation (POX) and autothermal reforming (ATR) of hydrocarbons.

Steam reforming uses thermal energy to separate hydrogen from the carbon components of hydrocarbons, and involves the reaction of these fuels with steam on catalytic surfaces. The first step of the reaction is the decomposition [6] of the fuel into hydrogen and carbon monoxide, followed by water gas shift reaction (WGS) of the carbon monoxide and water to carbon dioxide and hydrogen. Steam reforming is an endothermic process,

D. J. Moon (✉)
Clean Energy Research Center, Korea Institute of Science and Technology (KIST), 39-1, Hawolgok-dong Sungbuk-ku, Seoul, Republic of Korea
e-mail: djmoon@kist.re.kr

hence some of the fuel must be burned and the heat transferred to the reformer via heat exchangers.

Partial oxidation involves [7] the reaction of oxygen with fuel to produce H_2 and CO when the oxygen-to-fuel ratio is less than that required for total combustion. Partial oxidation can be conducted with a catalyst (catalytic partial oxidation) or without a catalyst (non-catalytic partial oxidation). The reaction rates are much higher for partial oxidation than for steam reforming, but the H_2 yield per carbon in the fuel is lower.

Autothermal reforming involves the reaction of oxygen, steam and fuel to produce H_2 and CO, and can be viewed as a combination of partial oxidation and steam reforming. This reforming step generates gases which contain 8–12% CO besides H_2, CO_2, CH_4 and air. This CO must be converted with the help of steam to CO_2 and hydrogen via WGS reaction to enrich the hydrogen [1, 2, 8].

The lack of an infrastructure for the production and distribution of H_2 has stimulated research in fuel processing, in particular, the development of fuel processors for reforming infrastructure fuels such as natural gas, liquefied petroleum gas (LPG), gasoline and diesel at the point of application.

Recently, proton exchanged membrane (PEM) fuel cells operating with hydrogen from hydrocarbon reforming technologies are being increasingly accepted as the most appropriate power source for future generation vehicles. It has polymer electrolyte and operates at 80 °C with hydrogen as reformate, prepared externally. For PEM fuel cells, the concentration of CO should be reduced as it poisons an anode catalyst. Solid oxide fuel cell (SOFC) is also gaining interest, though the operating temperature is high (700–900 °C). It has ceramic electrolyte and can use $H_2/CO_2/CH_4$ reformate as fuel which can be reformed internally or externally. It is tolerant to sulfur and there is no CO poison effect as observed in PEM fuel cells.

Steam reforming of hydrocarbons, especially of methane, is the largest and generally the most economical way to make hydrogen and has been reported by many researchers [6, 9–11]. Steam reforming gives the highest quantity of hydrogen in the product stream, but the requirements of considerable heat input, high catalyst loadings and large reactors are necessary. However, coupling this process with total oxidation by combusting part of the fuel can minimize the external energy demand to produce hydrogen efficiently in more compact reactors [12, 13]. Steam reforming of *n*-butane over supported Ni and Pt–Ni catalysts is reported [10] under conditions similar to fuel processing via indirect partial oxidation [13], i.e., the combination of total oxidation, steam reforming and water-gas shift reaction. Though supported nickel catalysts are used in industrially important reactions for producing hydrogen and synthesis gas from hydrocarbon feedstock [14–16], the problem of coke formation leading to the deactivation of nickel catalysts is often pointed out [17, 18].

In the last decade, attention has been paid on the production of synthesis gas by dry reforming of hydrocarbons like methane and propane [15, 19–22]. But CH_4 reforming by CO_2 is highly energy consuming and coke forming process [23, 24]. To solve this problem, an electrocatalytic internal reforming of CH_4 by CO_2 is reported [3–5, 20, 21] to coproduce a syngas and electricity in an SOFC system. This process is attractive from environmental and economical points of view because of the potential utilization of greenhouse gases as resources for the production of energy and high-value chemicals [1–5, 13].

Heterogeneous catalysts with Mg–Al hydrotalcite-like compounds as precursors and their utilization for CH_4 reforming were reported by Basini et al. [25, 26]. They focused the study on the Ni-based catalyst application in CH_4 partial oxidation and the effects of the residence time and the thermal profile were monitored to elucidate the catalytic reaction mechanism. Also, heterogeneous stoichiometric oxidation and catalytic partial oxidation of methane were studied [26] at the surfaces of MgO, γ-Al_2O_3, and CeO_2 containing small Rh clusters. Nonequilibrium oxidative conversion of methane to CO and H_2 with high selectivity and productivity over Ni/Al_2O_3 was reported at low temperatures [7]. Schmidt et al. reviewed [27] the issue about their work, investigating the catalytic partial oxidation of various hydrocarbons [28], the roles of the active metal species and the roughness of the surfaces [29], the effects of total pressure [30], and the effects of total flow rate [31]. Catalytic partial oxidation of hydrocarbons for generating hydrogen has gained much attraction due to its direct application in PEM fuel cells for generating clean electrical energy. The *spc*-Ni/MgAl catalysts were prepared starting from Mg–Al hydrotalcite-like compounds containing Ni at the Mg sites as precursors and successfully applied for the partial oxidation [32], steam reforming [11], and dry reforming [14, 19, 33–35]. Partial oxidation is an exothermic process which gives off heat. It is typically, a much faster process than steam reforming and requires a smaller reactor vessel. Partial oxidation process initially produces less hydrogen per unit of the input fuel than is obtained by steam reforming of the same fuel.

Partial oxidation reforming of fuels for vehicles was first proposed by Argonne National Laboratory (ANL) several years ago. For vehicle applications, POX reforming over SR is a low energy requirement and sulfur tolerance of catalyst. For hydrocarbon fuel reforming, a catalyst support must have a high surface area, must be stable at high temperatures, and possess a low pressure drop.

2 Features of Catalysts

2.1 Anode Supported Single Cell

Nickel is the most commonly used metal for SOFC anodes [36]. Since Ni catalyzes the formation of carbon filaments when exposed to hydrocarbons at SOFC operating temperatures, it is replaced with a different electronic conductor [37, 38]. Ni was replaced with Cu, since Cu is a poor catalyst for carbon formation [39, 40]. Because of the catalytic activity of ceria for the oxidation of hydrocarbon fuels, ceria is included in the anode to enhance anode performance [41, 42]. Cu–ceria–yttria-stabilized zirconia (YSZ) anodes are capable of direct, electrochemical oxidation of various fuels, including hydrocarbons that are liquids at room temperature [43, 44]. It is reported [39] that the anodes made from composites of Cu and yttria-stabilized zirconia (YSZ) perform very poorly unless ceria is added. More recently, direct oxidation of hydrocarbons at intermediate temperatures has been demonstrated with SOFC based on samaria doped ceria (SDC) electrolytes [45].

Lu et al. [46] replaced Cu with Au and observed similar electrochemical performance in direct oxidation SOFC system and demonstrated that ceria plays a crucial role in maintaining high performance in these direct-oxidation anodes.

We have studied [20] the performance of Ni–YSZ–CeO_2 and Ni–YSZ–MgO as anode catalysts (Table 1) for dry reforming of CH_4. Ni–YSZ–CeO_2 catalyst displayed higher reaction rate for the conversion of CO_2 and CH_4, 9.1 and 8.2 mmol/cm^2, respectively, than Ni–YSZ–MgO catalyst. It attained the maximum activity at above 800 °C. The BET surface area of both the catalysts after CH_4 reforming by CO_2 was found to increase by the deposition of carbon on the surface of the catalyst at high temperature with a decrease in the active metal surface area of catalysts due to the sintering of Ni. These catalysts along with NiO and YSZ were tested [4, 47, 48] for cogeneration of synthesis gas and electricity through internal reforming of CH_4 by CO_2 in SOFC system. Here, Ni–YSZ–CeO_2 catalyst too showed higher reaction rates than NiO–YSZ–MgO catalyst under the test conditions: temperature range = 650–850 °C; space velocity = 17,000 h^{-1}; and feed molar ratio of $CO_2/CH_4 = 1$. The power density in SOFC system increased almost threefold compared to other systems when the reactor design was modified to improve the contact between the cell and the current collector. This study showed that the performance of single cell in SOFC is significantly increased by the use of a suitable material and a proper design of the system. It was identified that Ni–YSZ–CeO_2 catalyst was deactivated by the formation of carbon on the surface of the catalyst within a few days.

Table 1 Structural properties of CH_4 reforming catalysts prepared for internal reforming of CH_4 by CO_2 in SOFC system

	BET surface area (m^2/g)		Total pore volume (cm^3/g)	Active metal surface area (m^2/g)
	Before	After^a		
NiO	1.34	0.32	0.006	0.246
YSZ	12.0	–	–	–
NiO–MgO	4.08	–	0.007	0.117
NiO–YSZ–MgO	8.9	13.4	0.003	0.081
MgO–YSZ–CeO_2	10.2	15.7	0.004	0.098

^{a} BET surface area of the catalysts after the dry reforming of CH_4 by CO_2

The TPR profiles of the Ni based catalysts used in the cogeneration of synthesis gas and electricity through internal reforming of CH_4 by CO_2 in SOFC system as listed in Table 1 is shown [2] in Fig. 1. NiO showed reduction peaks at about 380 and 580 °C. A weak reduction peak of CeO_2 was exhibited at about 800 °C, but YSZ did not show any reduction peak below 1,100 °C. A reduction peak at 380 °C for the NiO–YSZ based catalyst suggests that the NiO–YSZ based catalysts are active for reforming of CH_4 by CO_2. However, the active metal surface area over the NiO–YSZ–CeO_2 catalyst was higher than that of NiO–YSZ–MgO catalyst reflecting higher reforming activity.

2.2 Hydrotalcites

Hydrotalcites are based on the brucite structure, in which some magnesium is replaced by a trivalent cation such as aluminum (Al^{3+}), iron (Fe^{3+}) or chromium (Cr^{3+}). This replacement introduces a positive charge on the layered

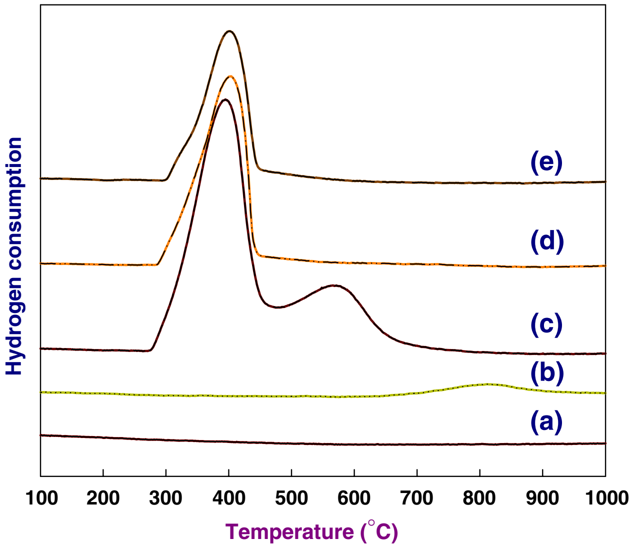

Fig. 1 TPR profiles of Ni based catalysts. (**a**) YSZ, (**b**) CeO_2, (**c**) NiO, (**d**) NiO–YSZ–CeO_2, (**e**) NiO–YSZ–MgO

double hydroxides (LDH), and this charge is counterbalanced by an anion that may be carbonate or sulphate. The interlayer anions can be incorporated to the structure during the synthesis process as well as in a later ionic exchange step. Hydrotalcites-like materials have been extensively studied [49–53] in last few decades for various catalytic applications such as steam reforming, base-catalyzed organic transformations, alcohol synthesis, alkylation of phenol with alcohols, selective oxidation, isomerization of allylic compounds and decomposition of nitrogen and sulfur oxides. Hydrotalcite-derived mixed oxides are used as ion exchangers, absorbers, catalysts and catalyst supports. They show interesting properties such as high surface area, "memory effect," phase purity, basic surface properties, and structural stability [54]. Upon calcinations, hydrotalcite-like compounds form a homogeneous mixture of oxides with a very small crystal size, stable to thermal treatment and upon reduction form small and thermally stable metal crystallites [6].

Usually, supported metal catalysts used in the reforming reactions of hydrocarbons are prepared by wet impregnation of different supports. But this method has drawbacks that it is not reproducible, gives inhomogeneity in metal distribution on surface and also fine metal particles tend to sinter at high temperature resulting in the catalyst deactivation [6]. So "solid phase crystallization" (*spc*) method giving stable and highly dispersed metal-supported catalyst using pervoskite [55–57] and hydrotalcite [19, 32] as precursor have been reported. Takehira et al. reported [6] *spc*-Ni/MgAl catalysts of various Mg/Al ratios, prepared from Mg–Al hydrotalcite-like compounds as the precursors and tested for steam reforming of CH_4 into synthesis gas, and compared with supported Ni catalysts prepared by impregnation. They concluded that *spc*-$Ni_{0.5}/Mg_{2.5}Al$ catalyst can be considered for the production of H_2 for polymer electrolyte fuel cells. *spc*-Ni/MgAl catalyst was also reported [19, 33, 34] to be successfully applied for partial oxidation [32], steam reforming [11] and dry reforming of CH_4 [33, 34].

Recently, we have reported our work [9, 58, 59] on steam reforming of *n*-hexadecane, a main constituent of diesel, over noble metal (Rh) modified Ni-based hydrotalcite catalyst. The catalysts were prepared by co-precipitation and dipping methods. The noble metal modified Ni-based hydrotalcite catalyst displayed higher resistance to the sintering of active metal than Ni-based hydrotalcite catalysts prepared by a conventional method. Rh modified Ni-based catalysts showed high resistance to the formation of carbon compared to the Ni-based catalysts. Hence, Rh modified Ni-based catalyst can be applied for the SR reaction of diesel.

The TPR profiles of catalysts prepared for SR of LPG are shown [9] in Fig. 2. All catalysts showed a reduction peak at about 800 °C, which may be due to the formation of Mg–Ni–O species. The NiO peak in hydrotalcite structure formed after dipping appeared at around 450 °C (Fig. 2a), which disappeared due to the formation of solid Mg–Ni–O solution upon calcination (Fig. 2b). Rh modified *spc*-Ni/MgAl catalysts displayed two peaks due to the reduction of Rh metal at 230 and 425 °C (Fig. 2c–e). These results reveal that the reduction and oxidation of Rh metal are easier than those of Ni metal, which agrees with the CO chemisorption and XRD data. This infers that Rh metal reacts with the oxygen source easier than Ni metal due to low reduction temperature and finally suppresses the sintering of Ni metal during the SR of *n*-hexadecane.

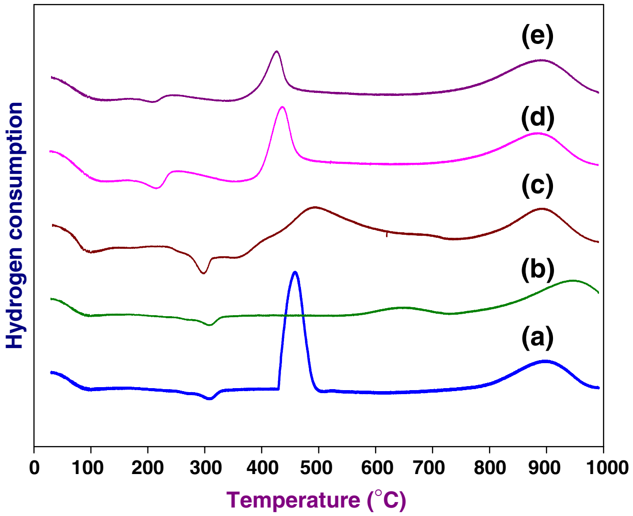

Fig. 2 TPR profiles of (**a**) *spc*-Ni/MgAl after dry at 60 °C for 12 h, (**b**) *spc*-Ni/MgAl after calcination at 850 °C, (**c**) 0.3 wt%Rh *spc*-Ni/MgAl after calcinations, (**d**) 0.5 wt%Rh *spc*-Ni/MgAl after calcination, (**e**) 1.0 wt%Rh *spc*-Ni/MgAl after calcination

2.3 Mixed Oxides

Velu et al. investigated [60] the oxidative steam reforming of methanol over a series of multi-component (Cu,Co,Zn,Al) mixed oxide catalysts. It was revealed that the Co free catalyst offered high H_2 production rates because of the presence of Co favors the CO hydrogenation reaction.

Newson et al. used [61] 1 wt%Rh on commercial mixed oxide for low-temperature POX reaction of low sulphur liquid hydrocarbons including refinery streams (C_4–C_{10}), at 500–600 °C instead of 900 °C [14, 62]. Since the concentration of CO in product gases was substantially lower, they eliminated the use of high- and low-temperature shift reactors (HTS, LTS) before the preferential oxidation (PROX) reactor.

We impregnated Ni using nickel nitrate solution on YSZ–CeO_2 and YSZ–MgO mixed oxides prepared by ball-mill technique to make our dry reforming catalysts such as

$NiO–YSZ–CeO_2$ and NiO–YSZ–MgO [20, 21]. $NiO–YSZ–CeO_2$ catalyst showed higher catalytic activity than NiO–YSZ–MgO catalyst, however, it was deactivated by the formation of carbon on the surface of the catalyst within a few days. The same $NiO–YSZ–CeO_2$ catalyst showed [63] a higher activity for tri-reforming of CH_4 without the formation of NiC phase than two commercial (ICI, HT) catalysts. It was reported that the sintering of nickel can be controlled by YSZ particles.

3 Catalytic Reforming of CH_4

3.1 Steam Reforming of CH_4

Today, most of hydrogen is produced by the steam reforming of methane source such as natural gas and byproduct of petroleum refining. In the steam reforming of methane, methane reacts with steam under 3–25 atm pressure in the presence of a catalyst to produce hydrogen, carbon monoxide and a relatively small amount of carbon dioxide. Steam reforming (Eq. 1) is an endothermic process, hence heat must be supplied to the process for the reaction to proceed.

Subsequently, water-gas shift reaction (Eq. 2) by which carbon monoxide and steam are reacted using a catalyst to produce carbon dioxide and more hydrogen. In a final process carbon dioxide and other impurities are removed from the gas stream, leaving essentially pure hydrogen. Steam reforming can also be used to produce hydrogen from other fuels, such as ethanol, propane, or even gasoline.

$$CH_4 + H_2O \rightarrow CO + 3H_2 \qquad \Delta H^{\circ}_{298} = 206.3\,\mathrm{kJ/mol} \qquad (1)$$

$$CO + H_2O \rightarrow CO_2 + H_2 \qquad \Delta H^{\circ}_{298} = -41.1\,\mathrm{kJ/mol} \qquad (2)$$

Natural gas reforming technology is advancing rapidly, and a natural gas pipeline delivery infrastructure already exists. The hydrogen produced from natural gas is used predominantly for petroleum refining and ammonia production for fertilizer.

Researchers still have targeted their research [6, 11] at developing a superior steam reforming catalyst to have application in fuel cell technology. Takehira et al. [6] reported that *spc*-Ni/MgAl catalysts prepared by co-precipitation method had high metal dispersion and hence higher activity for steam reforming of CH_4 into synthesis gas, compared with supported Ni catalysts prepared by impregnation. The *spc*-$Ni_{0.5}/Mg_{2.5}Al$ catalyst showed no deterioration in catalytic activity for 600 h even under a low steam to carbon ratio of 1.6, while a commercial $Ni/\alpha\text{-}Al_2O_3$ catalyst showed a clear decline in the activity. Metal supported catalysts prepared by a conventional wet impregnation method are not fully reproducible and may give rise to some inhomogeneity in the distribution of the metal on the surface of the support.

Recently, Takehira et al. reported [64], self-regenerative activity, by both trace Ru and Mg(Ni,Al)O periclase structure during daily start up and shut down (DSS) operation in steam reforming of CH_4. Trace Ru or RuNi alloy regenerates the Ni metal from Ni^{2+} in the periclase by hydrogen spillover and suppresses the deactivation of Ni/Mg(Al)O catalyst in the DSS SMR. Later on, they used [65] Rh-doped on Ni/Mg(Al)O catalyst and compared with that of Ru-doped catalyst for self activation and self regeneration of active metallic Ni particles. They observed better performance of Rh–Ni/Mg(Al)O catalyst over Ru–Ni/Mg(Al)O catalyst for self activation in stationary SMR as well as regenerative in the DSS SMR. Nagaoka et al. reported [66] CH_4 autothermal reforming with or without C_2H_6 over mono-(Ni/MgAl and Rh/MgAl) and bimetallic (Ni–Rh/MgAl) catalysts, having strong resistance of coke deposition. Higher activity for Ni–Rh/MgAl catalyst was observed under all tested condition than Rh/MgAl catalyst. Tomishige et al. modified [67] the surface of Ni catalyst with trace of Pt for oxidative steam reforming of CH_4. They found that Pt–Ni species maintain in the metallic state near the bed inlet. However, Ni species if used alone gets oxidized near the bed inlet in the presence of oxygen, causing decrease in the performance.

Recently, we reported [58, 68] *spc*-Ni/MgAl and 0.3 wt%Rh *spc*-Ni/MgAl catalysts that were used in the steam reforming of CH_4 for 53 h with H_2O/C ratio of 1/1. 0.3 wt%Rh *spc*-Ni/MgAl catalyst showed a higher CH_4 conversion (90%) than *spc*-Ni/MgAl catalyst (80%). The conversion decreased gradually over *spc*-Ni/MgAl catalyst whereas, for 0.3 wt%Rh *spc*-Ni/MgAl catalyst, the activity was found to be stable with time on stream up to 53 h.

3.2 Dry Reforming of CH_4

Since last decade, more attention has been paid to the production of synthesis gas using green house gases. The dry reforming of methane by carbon dioxide yielding a synthesis gas (Eq. 3) has received much interest because of the enhanced utilization of natural gas and greenhouse gases (namely CO_2 and CH_4) into highly valuable chemicals [35, 69, 70].

$$CH_4 + CO_2 \rightarrow 2CO + 2H_2 \qquad \Delta H^{\circ}_{298} = 247.3\,\mathrm{kJ/mol} \qquad (3)$$

However, two serious problems are associated with dry reforming of CH_4: deactivation of the catalyst by carbon formation and consumption of high energy due to endothermic process. For these reasons, various catalysts have been investigated for dry reforming of CH_4 by CO_2. Because of high cost and limited availability of noble metal catalysts such as Pt, Rh, and Ru [71–73], the commercialization of this process has been limited. Therefore, more work has been investigated over transition metal catalysts having reduced tendency of coke formation. For many years nickel-based catalysts have been proved to be the most suitable catalyst for hydrocarbon reforming. So nickel supported on oxides, such as Al_2O_3, MgO, TiO_2, ZrO_2, SiO_2, CeO_2 and La_2O_3 have been investigated [74–77] extensively as catalyst for the reforming of CH_4 by CO_2. The effects of the metal-supported interactions and acid–base properties of the supports on the catalytic activity and stability have been identified [78, 79]. However, research on nickel catalyst is still required in order to improve its coke resistance in the reforming of available hydrocarbons.

Catalysts prepared by conventional co-precipitation technique are used for partial oxidation of methane [25, 32] and propane [80] and dry reforming of methane [33]. Tsyganok et al. have reported [81] the introduction of nickel into Mg–Al LDH (layered double hydroxide) by a coprecipitation of Mg^{2+} and Al^{3+} with the pre-synthesized complex of Ni (II) with ethylenediaminetetraacetate, i.e., $[Ni\ (EDTA)]^{2-}$, where the chelated nickel species reside within interlayer space. Calcination of nickel introduced LDH in air yielded Ni–Mg–Al mixed oxide which upon reduction with hydrogen formed high, durable and reusable catalytic function toward dry reforming of methane [34]. Tsyganok et al. [81] observed high and sustainable catalytic activity and selectivity in the dry reforming of methane at 800 °C and also observed that LDH derived catalysts offered remarkably higher CH_4 and CO_2 conversions than those attained with catalysts prepared by sol–gel and cellulose template methods.

Direct dry reforming in the SOFC system is considered as an advanced process. Studies on the direct electrocatalytic oxidation of CH_4 were reported in a solid oxide fuel cell system with reasonable performance by Park et al. [82]. Ishihara et al. [83] reported their studies on the partial oxidation of methane over a fuel cell reactor for the simultaneous generation of synthesis gas and electric power.

To check the possibility of the development of a high performance electrode for application in an electrocatalytic internal reforming in the SOFC system, the catalytic reforming of CH_4 by CO_2 over Ni–YSZ modified catalysts, namely Ni–YSZ–CeO_2 and Ni–YSZ–MgO (Table 1) was investigated [20, 21]. Ni–YSZ–CeO_2 catalyst displayed higher reaction rate (9.1 mmol/cm^2) than Ni–YSZ–MgO catalyst (8.2 mmol/cm^2). Ni–YSZ–CeO_2 proved to be a promising catalyst to be used further in the internal and tri-reforming of CH_4 [5, 20, 21]. We also reported [3, 35–38] the electrocatalytic reforming of CH_4 by CO_2 in an SOFC system, co-producing a synthesis gas and electricity.

3.3 Tri-Reforming of CH_4

Comparatively, the tri-reforming is much easier process for protecting carbon formation than dry reforming process. It is a combination of endothermic CH_4 reforming (Eq. 4), steam reforming (Eq. 1) and exothermic oxidation of CH_4 (Eqs. 5 and 6), which has more importance in regard to both industrial and environmental aspect [84–86].

$$CH_4 + CO_2 \rightarrow 2CO + 2H_2 \qquad \Delta H^{\circ}_{298} = 247.3\,\text{kJ/mol} \tag{4}$$

$$CH_4 + {}^1\!/\!{}_2O_2 \rightarrow CO + 2H_2 \qquad \Delta H^{\circ}_{298} = -35.6\,\text{kJ/mol} \tag{5}$$

$$CH_4 + 2O_2 \rightarrow CO_2 + 2H_2O \qquad \Delta H^{\circ}_{298} = -880\,\text{kJ/mol} \tag{6}$$

During tri-reforming reaction, many kinds of side reactions for the formation (Eqs. 7 and 8) and destruction (Eqs. 9–11) of coke occurred simultaneously.

$$CH_4 \rightarrow C + 2H_2 \qquad \Delta H^{\circ}_{298} = 74.9\,\text{kJ/mol} \tag{7}$$

$$2CO \rightarrow C + CO_2 \qquad \Delta H^{\circ}_{298} = -172.2\,\text{kJ/mol} \tag{8}$$

$$C_{(ads)} + CO_2 \rightarrow 2CO \qquad \Delta H^{\circ}_{298} = 172.2\,\text{kJ/mol} \tag{9}$$

$$C_{(ads)} + H_2O \rightarrow CO + H_2 \qquad \Delta H^{\circ}_{298} = 131.4\,\text{kJ/mol} \tag{10}$$

$$C_{(ads)} + O_2 \rightarrow CO_2 \qquad \Delta H^{\circ}_{298} = -393.7\,\text{kJ/mol} \tag{11}$$

Previously, we reported [3, 4, 20, 87] that NiO–YSZ–CeO_2 catalyst showed better catalytic performance than NiO–YSZ–MgO in dry reforming of CH_4 by CO_2. But it was deactivated by the formation of carbon on the surface of catalyst within few days. Based on the previous results, we have reported [69] the production of synthesis gas by tri-reforming of CH_4 over NiO–YSZ–CeO_2 catalyst and compared the catalyst with two commercial steam reforming catalysts procured from Imperial Chemical Industry (ICI) Co. (ICI 57-7) and Holder Topsoe Co. (HT R67).

Figure 3 represents the comparison of the out-gas distribution for tri-reforming reaction over the NiO–YSZ–CeO_2 and commercial steam reforming catalysts and dry reforming reaction over NiO–YSZ–CeO_2 catalyst. The conversions of CO_2 and CH_4 in the tri-reforming of CH_4 were 100% with the production of quantitative amounts of H_2 and CO. However, the conversions of CO_2 and CH_4 in the dry reforming were 92% and 100%, respectively. The catalytic activity for the tri-reforming reaction over NiO–YSZ–CeO_2 catalyst was higher than for dry reforming.

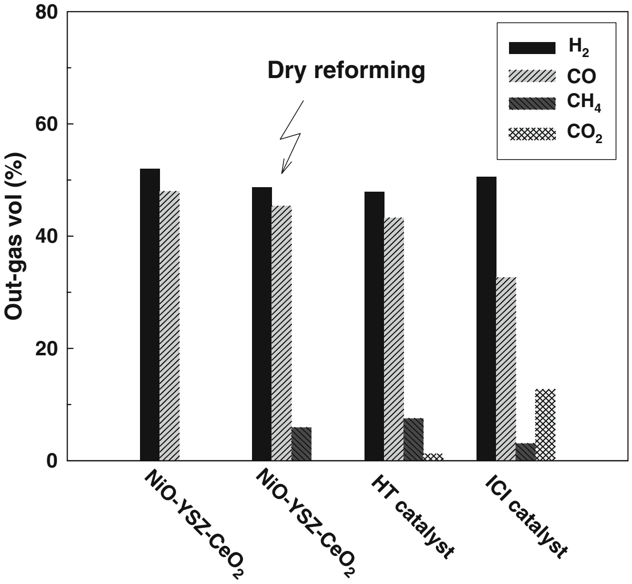

Fig. 3 The comparison of the out-gas distribution for the tri-reforming of CH_4 over various catalysts. The tri-reforming reaction was carried out at the temperature of 800 °C, feed molar ratio of $CH_4:CO_2:O_2:H_2O = 1:1:0.1:1$ and GHSV of 10,000 h^{-1}. The dry reforming was performed at a feed molar ratio of $CH_4/CO_2 = 1$ and GHSV of 17,000 h^{-1}

Also, NiO–YSZ–CeO_2 catalyst showed a higher tri-reforming activity than the commercial catalysts under the same reaction conditions.

As seen in Fig. 4, no NiC phase was detected on the surface of NiO–YSZ–CeO_2 catalyst after tri-reforming reaction, like after dry reforming reaction. Tri-reforming of CH_4 was found to be more desirable than dry-reforming reaction over NiO–YSZ–CeO_2 catalyst. It was also reported that the product ratio of H_2/CO can be controlled by the tri-reforming of CH_4. The results suggest that the synthesis gas produced by the tri-reforming of CH_4 can be used for the production of DME, Fischer–Tropsch synthesis fuels and high-valued chemicals [88–90] and applied to the fuel processor of SOFC and MCFC systems.

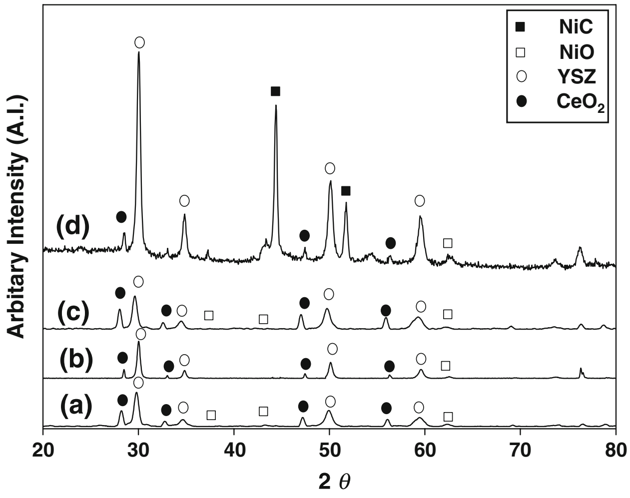

Fig. 4 The XRD patterns of NiO–YSZ–CeO_2 catalysts (**a**) before reduction, (**b**) after reduction, (**c**) after the tri-reforming reaction for 120 h and (**d**) after dry reforming reaction. The reaction was carried out at the reaction temperature of 800 °C, feed molar ratio of $CH_4:CO_2:O_2:H_2O = 1:1:0.1:1$ and GHSV of 10,000 h^{-1}

3.4 Internal Reforming of CH_4 by CO_2 in SOFC System

To solve the problem of the deactivation of the catalyst in dry reforming of CH_4, the internal reforming of CH_4 by CO_2 was carried out in a SOFC system using Ni-based anode catalysts, which showed a higher catalytic activity in the dry reforming of CH_4.

We reported [3, 91, 92] the cogeneration of a syngas and electricity by the electrocatalytic reforming of CH_4 by CO_2 in a SOFC system using NiO and NiO–MgO catalysts. These catalysts were prepared by a precipitation method using nitrates and ammonium hydroxide at pH 9, followed by aging the precipitates at room temperature for 24 h, filtration, dried at 100 °C and calcined at 900 °C for 6 h. The single cell was prepared by a tape casting method. NiO–MgO catalyst exhibited higher reaction rates than NiO catalyst under the experimental conditions. However, the reaction rates of CO_2 and CH_4 decreased more drastically over NiO catalyst than on NiO–MgO catalyst. The BET surface area and the total pore volume of NiO catalyst were found to be decreased by 76% and 80%, respectively, after the reaction due to the sintering of Ni.

Figure 5 shows the reaction rates of CH_4 and CO_2 and the current density over the electrocatalytic cell (NiO–

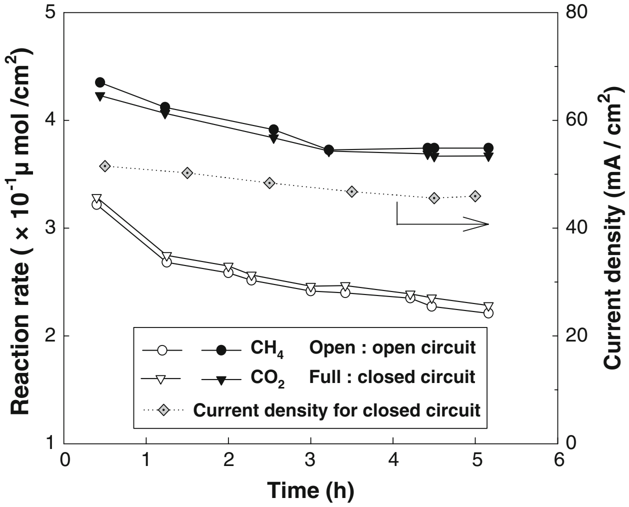

Fig. 5 The reaction rates of CH_4 and CO_2 and the current density over the electrocatalytic cell (NiO–MgO|YSZ|(La,Sr)MnO_3) with a time on stream

MgO|YSZ|(La,Sr)MnO_3) with time on stream under the open and closed circuit conditions. The eletrocatalytic reforming reaction in SOFC system was carried out at atmospheric pressure and a temperature of 800 °C. The reaction rates of CH_4 and CO_2 under the open-circuit condition were found to be lower than under the closed-circuit condition. The rates of CH_4 and CO_2 and the current density under the closed-circuit condition were stable after the electrocatalytic reaction for 3 h whereas those of CH_4 and CO_2 under the open-circuit condition slowly decreased due to the deposition of coke. The catalyst electrode under the closed circuit was stable during the electrocatalytic reforming of CH_4 by CO_2 because of the fast removal of coke deposition due to oxygen ion flux under the closed-circuit condition. The selectivities of CO_2 and CO under the closed circuit condition were 28.9 and 13.1%, respectively, whereas those of CO_2 and CO under open circuit were 14.8 and 18.59%. The amount of coke under the open-circuit condition was 120 mg C/$g_{catalyst}$ after 5 h, but the amount of coke under the closed-circuit condition drastically decreased compared to that under the open-circuit condition.

The mechanism of CH_4 reforming by CO_2 over noble based catalysts was proposed to consist of several steps [60–62]. It can be produced by CH_4 decompositions (Eqs. 12–16), CO_2 disproportionation (Eq. 17) and partial oxidation of surface carbon (Eq. 18). Also, surface carbon can be produced by methane decomposition (Eq. 19) and CO disproportionation (Eq. 20).

$$CH_4 \rightarrow CH_3(ads) + H(ads) \tag{12}$$

$$CH_3(ads) \rightarrow CH_2(ads) + H(ads) \tag{13}$$

$$CH_2(ads) \rightarrow CH(ads) + H(ads) \tag{14}$$

$$CH(ads) \rightarrow C(ads) + H(ads) \tag{15}$$

$$CH_4 \rightarrow C(ads) + 2H_2 \tag{16}$$

$$CO_2 \rightarrow CO(ads) + O(ads) \tag{17}$$

$$C(ads) + O(ads) \rightarrow CO \tag{18}$$

$$CH_4 \rightarrow C(ads) + 2H_2 \qquad (\Delta H^{\circ}_{298} = 74.9\,\text{kJ/mol}) \tag{19}$$

$$2CO \rightarrow C(ads) + CO_2 \qquad (\Delta H^{\circ}_{298} = -172.4\,\text{kJ/mol}) \tag{20}$$

In the electrochemical cell, oxygen ions (O^{2-}) are formed on the counter electrode according to the following reaction (Eq. 21):

$$0.5O_2 + 2e^- \rightarrow O^{2-} \tag{21}$$

These oxygen ions are transferred to the catalyst electrode through the YSZ electrolyte. The possible electrolytic reactions with the oxygen ions transferred to the catalyst electrode occur by the following reactions (Eqs. 22–25):

$$CO + O^{2-} \rightarrow CO_2 + 2e^- \tag{22}$$

$$H_2 + O^{2-} \rightarrow H_2O + 2e^- \tag{23}$$

$$Cs + O^{2-} \rightarrow CO + 2e^- \tag{24}$$

$$Cs + 2O^{2-} \rightarrow CO_2 + 4e^- \tag{25}$$

Carbon deposition was prevented by the reaction (Eqs. 24 and 25) of the surface carbon with the oxygen ion transferred from cathode electrode in SOFC system.

Figure 6 shows [91, 92] the performance of current voltage and power density with current density in the electrocatalytic cell (NiO–MgO|YSZ|(La,Sr)MnO_3) when CH_4 and CO_2 were used as reactants. The open-circuit voltage (OCV) obtained for the single cell at 800 °C and atmosphere was 0.96 V, which was lower than the theoretical (V = 1.24) OCV. The maximum power density was at 30 mA. The electricity can be produced by the electrochemical reactions such as the oxidation of CO and H_2 (Eqs. 22 and 23), surface carbon (Eqs. 24 and 25), and CH_4 (Eqs. 26 and 27).

$$CH_4 + O^{2-} \rightarrow CO + 2H_2 + 2e^- \tag{26}$$

$$CH_4 + 4O^{2-} \rightarrow CO_2 + 2H_2O + 8e^- \tag{27}$$

For H_2 as reactant, the electricity was produced by the electrochemical reaction (Eq. 13). In our study the OCV obtained for the single cell tested at 800 °C and atmosphere was 1.04 V. Ni-based catalysts were found to be suitable as the electrode of SOFC in terms of the voltage-power performance.

In our later work [4], we have investigated CH_4 reforming by CO_2 over NiO–YSZ based anode catalysts for application to a single cell in SOFC. Anode catalyst

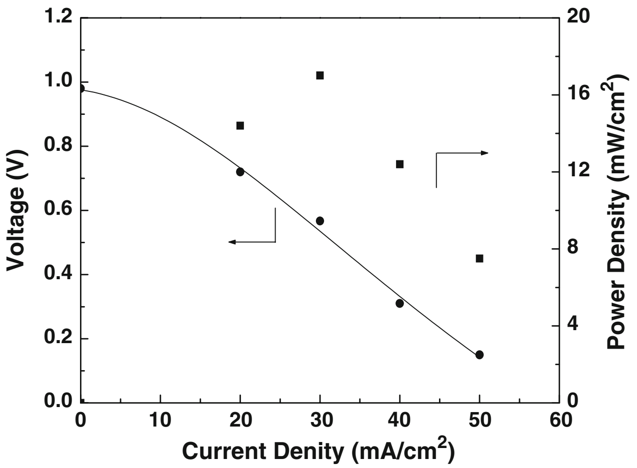

Fig. 6 The performance of current voltage and power density with current density in the electrochemical cell (NiO–MgO|YSZ|(La,Sr)MnO_3) at 800 °C

materials were prepared through a physical mixing method using NiO (Aldrich), YSZ (Tosoh Co.), MgO (Nakarai Chemicals) and CeO_2 (Aldrich). Initially, powders of NiO, YSZ, MgO or CeO_2 were mixed by dry ball milling using a zirconia ball for 24 h, and then the powder mixture was ground in a mortar until fine powders were obtained. Cathode materials were prepared through the maleic acid method using nitrates of La, Sr and Mn. These chemicals were dissolved in distilled water with maleic acid and pH was adjusted with NH_4OH. The solution was heated at 100 °C for 6 h, followed by drying in an oven at 210 °C and calcining at 800 °C for 2 h in air. The single cell was prepared by using a tape casting method. We carried out catalytic reforming of CH_4 by CO_2 in a fixed bed reactor in a temperature range of 650–850 °C. The internal reforming of CH_4 by CO_2 was performed using an electrochemical cell in the SOFC system at 800 °C and in atmospheric air under open and closed circuit conditions.

The conversions of CO_2 and CH_4 over NiO–YSZ–MgO and NiO–YSZ–CeO_2 catalysts with time on stream are illustrated in Fig. 7. The catalytic activity and selectivity over both catalysts were also very stable during the entire reaction. The conversions of CO_2 and CH_4 over the NiO–YSZ–CeO_2 catalyst were 100% and 80%, respectively, which were slightly higher than those over NiO–YSZ–MgO. The result mainly attributes to the better metal dispersion on NiO–YSZ–CeO_2, which is supported by chemisorption and SEM data. XRD of these catalysts before and after the reaction (Fig. 8) shows the formation of NiC from NiO after the reaction for 5 h.

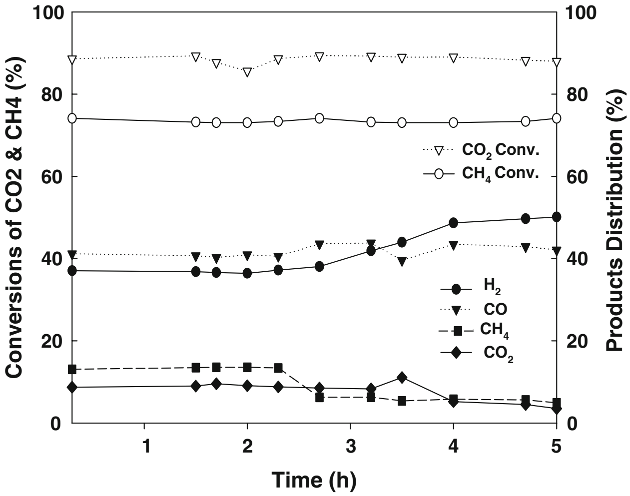

(a) NiO-YSZ-MgO

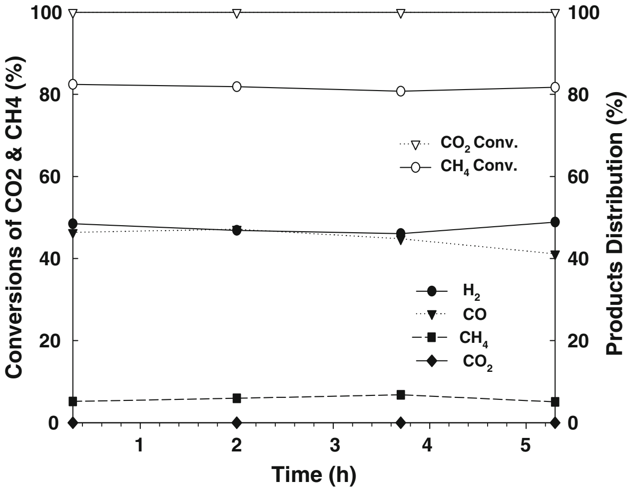

(b) NiO-YSZ-CeO_2

Fig. 7 The effect of time on stream on the conversions of CO_2 and CH_4 for catalytic CH_4 reforming by CO_2

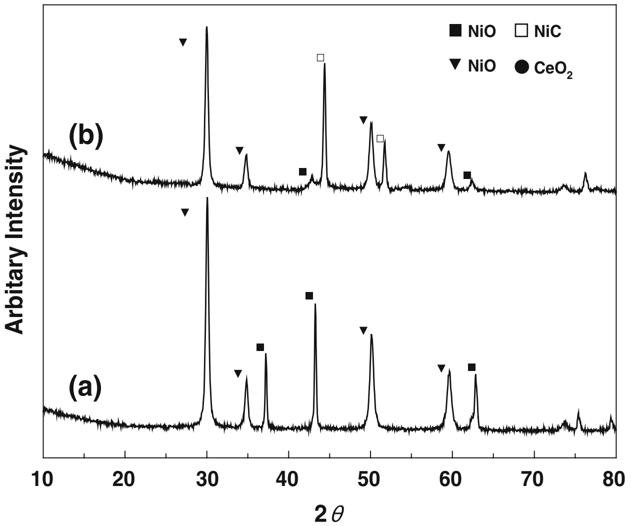

(a) NiO-YSZ-MgO

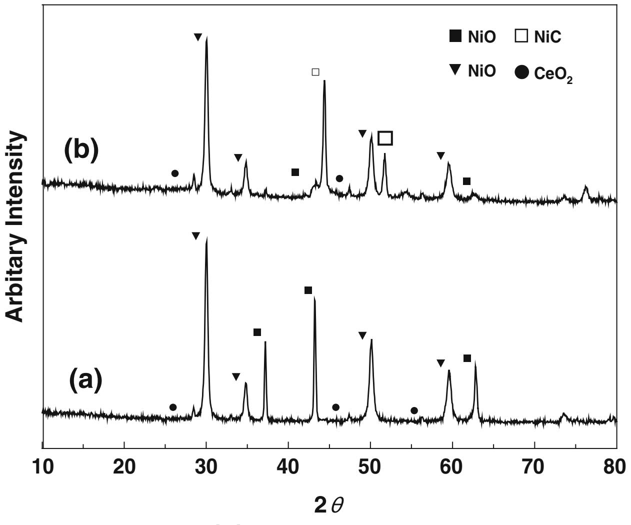

(b) NiO-YSZ-CeO_2

Fig. 8 XRD patterns of NiO–YSZ–MgO and NiO–YSZ–CeO_2 catalysts before (**a**) and after (**b**) the catalytic reforming of CH_4 by CO_2 in fixed bed reactor

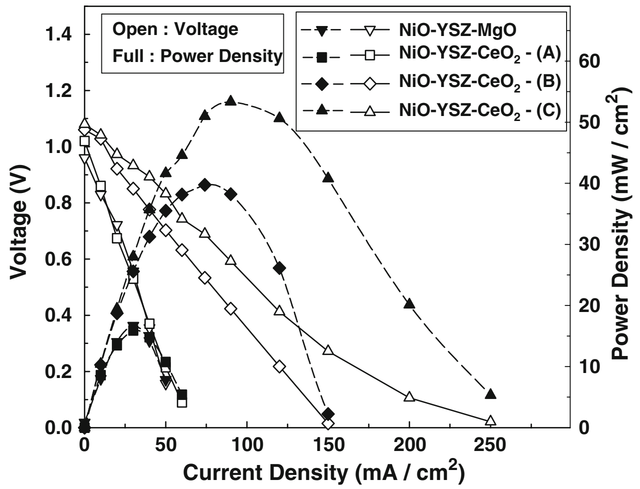

Fig. 9 The performance of current voltage and power density with current density in the electrochemical cells (different anode|YSZ|(La,Sr)MnO_3) at 800 °C when CH_4 (50 vol%) and CO_2 (50 vol%) were used as reactants. Flow rates of reactants and air are 20 mL/min, respectively

The reaction rates of CH_4 and CO_2 and current density under closed circuit conditions were stable whereas those of CH_4 and CO_2 under open circuits decreased slowly. Changes in the voltage and power density with the current density of the electrocatalytic cells (different anode|YSZ|(La,Sr)MnO_3) at 800 °C are illustrated in Fig. 9. In one of three methods employed, for case C, the reactor design was modified to improve the contact between the cell and the current collector. An optimized load by metal weight (0.16 N cm^{-2}) was placed on the reactor. This modified SOFC systems designed in case C, showed significantly improved electrical performance better than in the other systems. The open-circuit voltage over the single cell (NiO–YSZ–CeO_2|YSZ|(La,Sr) MnO_3) was 1.1 V; a power density of 54 mW/cm^2 was obtained at a current density 100 mA/cm^2. As shown in Fig. 9**,** the power density of the modified SOFC system (case C) was increased almost threefold relative to that of the initial system (case A).

The results suggest that the internal reforming of CH_4 by CO_2 in SOFC system can be applied for the production of a syngas and electricity as a sequestration technology of greenhouse gases.

4 Catalytic Reforming of LPG

Steam reforming of LPG is not much studied in open literature. However, coke formation over Ni and Ni–Mo catalysts during *n*-butane steam reforming [93, 94], activity/selectivity features of Ni, Pd and Pt catalysts and steam reforming kinetics of various hydrocarbons over Ni catalysts are reported [95, 96]. Avci et al. studied [97] the ignition characteristics of *n*-butane over monometallic Ni/δ–Al_2O_3 and bimetallic Pt–Ni/δ-Al_2O_3 catalysts under the conditions pertinent to fuel processor operation in the fuel-rich regime. They obtained lower reaction temperatures by the addition of a small amount of Pt to Ni, indicating the possibility of initiating the hydrogen-generating indirect partial oxidation route with lower energy requirement. Although monometallic Ni catalysts are best steam reforming catalysts, they are not superior in indirect partial oxidation due to their limited total oxidation activity and their deactivation tendency via oxidation. So later on Avci et al. studied [10] the steam reforming of *n*-butane over Ni/δ-Al_2O_3 and Pt–Ni/δ-Al_2O_3 catalysts at temperatures between 305 and 405 °C. Though both catalysts demonstrate similar trends in activities and in product formation rates without the formation of coke and carbon monoxide at a ratio of $H_2O/C = 3$, carbon monoxide was found to be produced only around 405 °C with low rates. The Pt–Ni catalyst exhibited superior performance at 405 °C where *n*-butane is completely converted and at 355 °C where hydrogen to methane point selectivity is maximized indicating the presence of a synergistic interaction between Pt and Ni sites.

Steam reforming of LPG (Eqs. 28–30) is mainly investigated [59, 97–102] over noble metal catalysts (e.g. Rh, Ru and Pt) on oxide supports.

Table 2 Characteristic of catalysts prepared for steam reforming of LPG

Catalyst	Molar ratio (Ni + Mg)/Al	BET surface area[a] (m^2/g)	Total pore volume[a] (cm^3/g)	Active metal surface area[b] (m^2/g)
spc-Ni/MgAl-A	1	171.1	0.245	11.54
spc-Ni/MgAl-B	2	184.2	0.258	12.07
spc-Ni/MgAl-C	3	197.7	0.285	13.02
spc-Ni/MgAl-D	4	190.3	0.273	13.02
spc-Ni/MgAl-E	5	188.5	0.269	12.31
spc-Ni/MgAl-F	6	186.4	0.264	12.15
0.3 wt%Ru *spc*-Ni/MgAl	3	107.7	0.373	10.41
0.3 wt%Rh *spc*-Ni/MgAl	3	105.4	0.375	10.35

[a] Derived from N_2 physisorption

[b] Derived from CO chemisorption

$$C_3H_8 + 3H_2O \rightarrow 7H_2 + 3CO \qquad 497.7\ \text{kJ/mol} \qquad (28)$$

$$C_4H_{10} + 4H_2O \rightarrow 9H_2 + 4CO \qquad 649.9\ \text{kJ/mol} \qquad (29)$$

$$(3C_3H_8 + 7C_4H_{10}) + 37H_2O \rightarrow 84\ H_2 + 37CO \qquad (30)$$

The major difficulty in the reforming of LPG is the degradation of the reforming catalyst due to the possible carbon deposition from the decomposition of hydrocarbons, particularly at high temperatures. Reforming of LPG over Ru/CeO_2–Al_2O_3 catalyst with a low inlet steam requirement at 450 °C is reported by Suzuki et al. [99]. The main products formed from the steam reforming of LPG are hydrogen, carbon monoxide and carbon dioxide, however the formation of ethane, ethylene and methane are usually observed due to the decomposition of LPG and methanation reactions. It is reported [97, 100] that an autothermal reforming process using added oxygen together with LPG and steam provides great benefits in terms of catalyst stability, low coke formation, and elimination of the formation of higher hydrocarbons (i.e. C_2H_6 and C_2H_4). High reforming reactivity with low carbon formation over Pt/CeO_2 is reported by Recupero et al. [59]. Recently, several researchers reported [103, 104] high activity for the reforming reactions with excellent resistance to carbon formation over precious metals (Pt, Rh and Ru) based catalysts. However, taking into account of the high prices of these metals for commercial usage, an alternative ceria based catalyst is developed by many researchers [105, 106], based on the ideas of high oxygen mobility (redox property) [107], high oxygen storage capacity [108–110], strong metal to support interaction [111] and modifiable capability [110].

Laosiripojana et al. reported [105] steam and autothermal reforming reactions of LPG over high surface area CeO_2 synthesized by surfactant-assisted approach, which were studied under SOFC operating conditions. This catalyst due to its redox property provides significantly higher reforming reactivity and excellent resistance toward carbon deposition compared to the conventional Ni/Al_2O_3 catalyst. The gas–solid reaction between the hydrocarbons present in the system and lattice oxygen takes place at ceria surface during reforming process. Oxygen contained in the autothermal reforming reactant stream reduced the degree of carbon deposition by eliminating the formation of higher hydrocarbons like ethane, ethylene.

We reported [68] the high and stable activity of Ni-loaded catalysts prepared from Mg–Al hydrotalcite–like anionic clay for steam reforming of LPG. The concentration of H_2 after 5 h was nearly the same over *spc*-Ni/MgAl and ICI

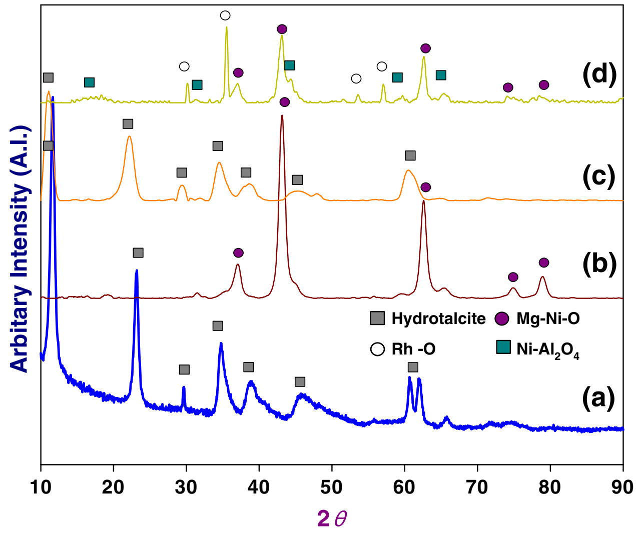

Fig. 10 XRD patterns of hydrotalcite (Mg–Al) and 0.3 wt%Rh *spc*-Ni/MgAl catalysts prepared by dipping method

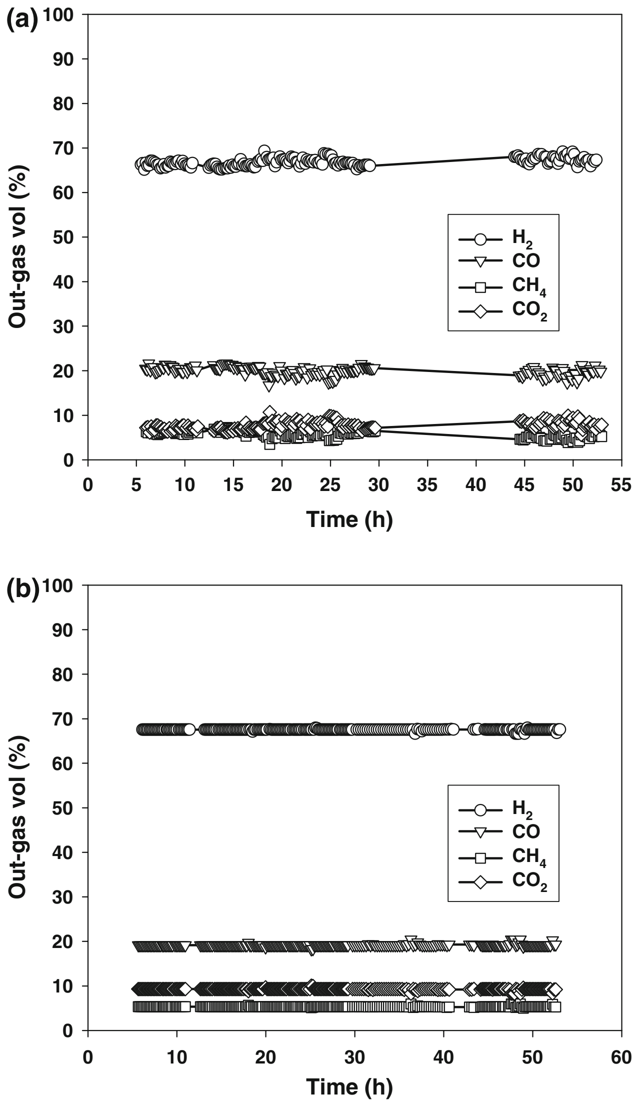

Fig. 11 Product distributions of (**a**) 0.3 wt%Ru *spc*-Ni/MgAl and (**b**) 0.3 wt%Rh-*spc*-Ni/MgAl catalysts for steam reforming of LPG on time on stream up to 53 h. Reaction conditions: temperature = 700 °C, GHSV = 20,000 h^{-1} and $H_2O/C = 1.0$

catalysts for SR of LPG. The concentration of H_2 was maintained during reaction time (186 h) at 800 °C, GHSV = 20,000 h^{-1} with $H_2O/C = 2$. However, it decreased over commercial ICI catalyst due to the formation of carbon. The 'memory effect' property of hydrotalcite-like support is believed to allow the reconstruction of the original hydrotalcite structure under mild conditions when contacting the product of the thermal treatment contacts with water which minimizes the degradation of the catalyst during steam reforming reaction.

Steam reforming of LPG over nickel-based and noble-metal-modified nickel-based catalysts (Table 2) using (different Ni to Mg ratio) hydrotalcite-like support is reported [58, 68, 112, 113] recently. *spc*-Ni/MgAl catalyst was prepared by a co-precipitation method and later modified with noble metals (Ru,Rh) by a dipping method. Among the non-impregnated Ni-based catalysts, *spc*-Ni/MgAl–C catalyst shows good performance up to 186 h for steam reforming of LPG, though later on the activity was found to be declined at 800 °C, $H_2O/C = 2$ and GHSV = 20,000 h^{-1}. Figure 10 shows the XRD patterns of hydrotalcite (Mg–Al) and 0.3 wt%Rh *spc*-Ni/MgAl catalysts prepared by a dipping method. XRD pattern (a) is typical hydrotalcite peak pattern taken after drying at 60 °C for 12 h in air. Then after calcining at 850 °C for 5 h, hydrotalcite structure changed to Mg–Ni–O crystalline form (b). When Rh modified *spc*-Ni/MgAl catalyst was prepared using *spc*-Ni/MgAl by a dipping method followed by drying at 80 °C for 6 h, Mg–Ni–O structure was found to reconstitute to hydrotalcite by memory effect (c). XRD pattern (d) shows that loaded Rh forms Rh_xO_x on the surface of Rh-modified *spc*-Ni/MgAl catalyst prepared by a dipping method. Figure 11 shows the product distributions of noble-metal-modified Ni-based catalysts for steam reforming reaction with time on stream up to 53 h at reaction conditions: temperature = 700 °C, GHSV = 20,000 h^{-1} and $H_2O/C = 1.0$. Ru modified *spc*-Ni/MgAl catalyst showed H_2: 64–66%, CH_4: 5–7%, CO: 18–21%, CO_2: 6–10% product distribution by vol(%) whereas Rh modified *spc*-Ni/MgAl catalyst formed H_2: 67%, CH_4:

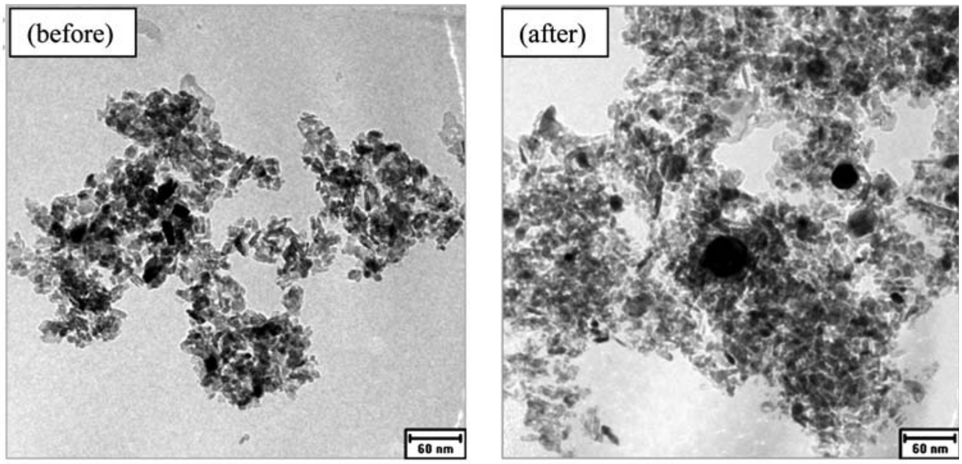

(a) **0.3wt% Rh *spc*-Ni/MgAl catalyst**

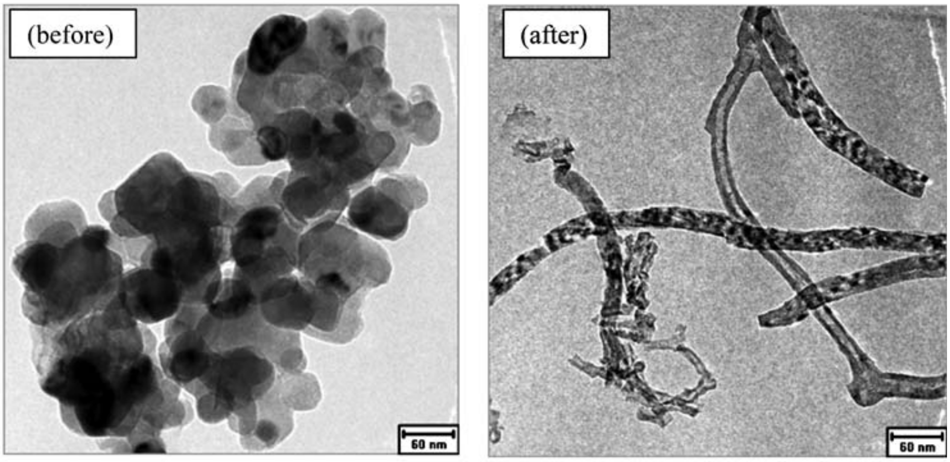

(b) **0.3wt% Ru *spc*-Ni/MgAl catalyst**

Fig. 12 TEM images of 0.3 wt%Ru *spc*-Ni/MgAl and 0.3 wt%Rh *spc*-Ni/MgAl catalysts before and after the steam reforming of LPG

4.9%, CO: 19%, CO_2: 8% by vol(%). It was found that Rh loaded catalyst showed stable performance for the SR of LPG without fluctuation in product distribution under severe reaction conditions: temperature = 700 °C, GHSV = 20,000 h^{-1}, H_2O/C = 1.0.

Figures 12 and 13 shows the TEM images and TGA profiles of 0.3 wt%Ru *spc*-Ni/MgAl and 0.3 wt%Rh *spc*-Ni/MgAl catalysts, respectively, before and after the reaction. As seen in TEM micrographs, plenty of carbon was formed on Ru *spc*-Ni/MgAl catalyst, during the reaction, compared to Rh *spc*-Ni/MgAl catalyst. The TGA profiles also show more weight loss for Ru *spc*-Ni/MgAl catalyst compared to Rh *spc*-Ni/MgAl catalyst, which agrees well with the TEM data. This infers that Ru metal is not effective for the inhibition of carbon formation. It was concluded that the addition of Rh metal to *spc*-Ni/MgAl enhanced the activity for LPG reforming and constrained the carbon deposition. Also 0.3% Rh *spc*-Ni/MgAl catalyst was found to have prolonged stability up to 1,100 h in the steam reforming of LPG as seen in Fig. 14. These results draw a conclusion that 0.3 wt%Rh *spc*-Ni/MgAl catalyst is a desirable LPG SR catalyst for application in hydrogen station and fuel processor systems. *spc*-Ni/MgAl catalyst displayed a better activity than ICI commercial CH_4 SR catalyst, but had a tendency to coke formation even though carbon formed did not affect adversely in this reaction. It was found that 0.3 wt%Rh *spc*-Ni/MgAl catalyst showed the strong restraint of carbon formation compared to 0.3 wt%Ru *spc*-Ni/MgAl catalyst.

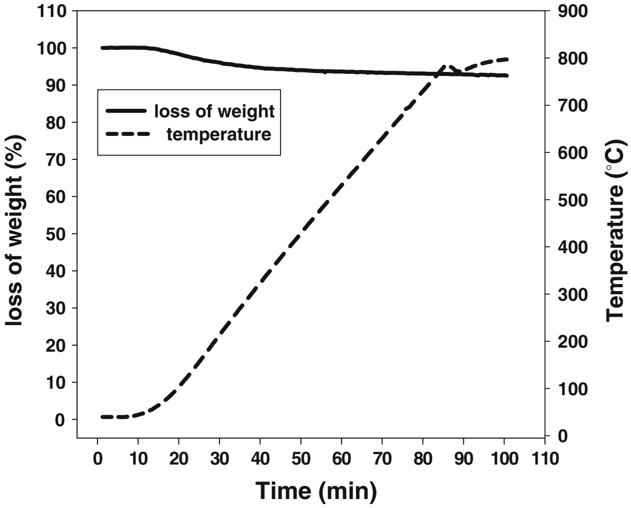

(a) 0.3wt% Rh *spc*-Ni/MgAl

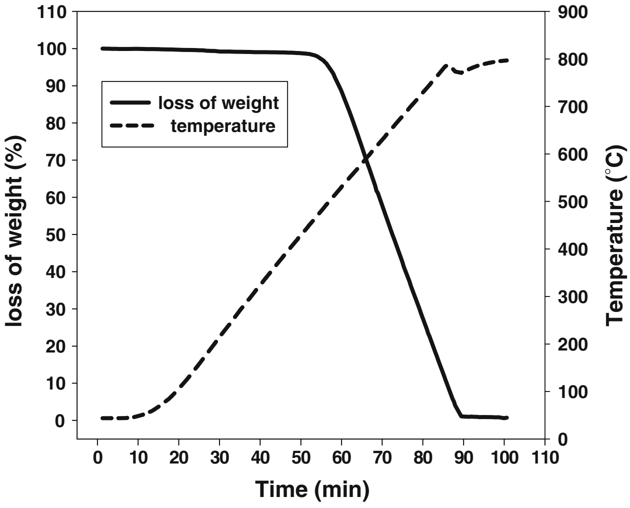

(b) 0.3wt% Ru *spc*-Ni/MgAl

Fig. 13 TGA profiles of 0.3 wt%Ru *spc*-Ni/MgAl and 0.3 wt%Rh *spc*-Ni/MgAl catalysts before and after the steam reforming of LPG

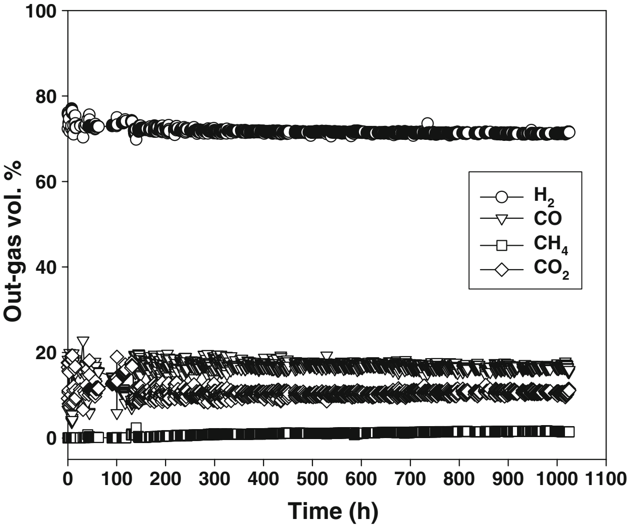

Fig. 14 Long term stability of 0.3% Rh *spc*-Ni/MgAl catalyst in the steam reforming of LPG

5 Conclusions and Future Directions

This review compiled the work carried out in this laboratory for the production of hydrogen by catalytic reforming of gaseous hydrocarbons fuels such as methane, propane, butane and LPG.

We have investigated CH_4 reforming by CO_2 over NiO–YSZ based catalyst which can be a suitable anode catalyst for application to a single cell in SOFC. For the dry reforming of CH_4 by CO_2, NiO–YSZ–CeO_2 catalyst was found to be active, but was deactivated due to carbon deposition after long run [3, 20, 87]. The same catalyst has shown higher activity and resistance to carbon deposition in the tri-reforming of CH_4, unlike in the dry reforming reaction [5]. Tri-reforming of CH_4 is more desirable than dry-reforming reaction over NiO–YSZ–CeO_2 catalyst for application to SOFC and MCFC fuel processor systems and for the production of high-valued chemicals such as methanol, hydrocarbons, dimethyl ether and the syngas production by GTL process [3–5, 88, 92]. But more studies on long term stability test, scale-up of the catalysts, and carbon dioxide sequestration are needed. We also reported the cogeneration of a syngas and electricity by the electrocatalytic reforming of CH_4 by CO_2 in SOFC system using Ni-based anode catalyst such as NiO–MgO, NiO–MgO–CeO_2 and NiO–YSZ–CeO_2. We overcome the shortcomings associated with the catalytic deactivation due to carbon deposition and the high-energy consumption.

We developed 0.3 wt%Rh *spc*-Ni/MgAl catalyst for steam reforming of LPG to be applied in hydrogen station and fuel processor systems. The addition of Rh to *spc*-Ni/MgAl catalyst restricted the deactivation of the catalyst due to the carbon formation in steam reforming of LPG and also renders long-term stability to the catalyst under tested conditions. It was found [9] that addition of Rh metal to the *spc*-Ni/MgAl catalyst had a promoting effect by inhibiting the sintering of Ni metal particles under tested conditions. 0.3 wt%Rh *spc*-Ni/MgAl catalyst showed the strong restraint of carbon formation compared to 0.3 wt%Ru *spc*-Ni/MgAl catalyst. 0.3% Rh *spc*-Ni/MgAl catalyst had a prolonged stability for more than 1,100 h in the steam reforming of LPG.

Acknowledgements Author would like to thank our coworkers for their valuable research contributions in reforming of gases hydrocarbons summarized in this review. The author would also like to acknowledge financial support from KIST, SK Energy and H_2FC to carry out this research in Clean Energy Research Center, Korea Institute of Science and Technology (KIST).

References

1. Moon DJ, Sreekumar K, Lee SD, Lee BG, Kim HS (2001) Appl Catal A: Gen 215(1–2):1
2. Moon DJ, Ryu JW (2003) Catal Today 87:255
3. Moon DJ, Park JM, Kang JS, Yoo KS, Hong SI (2006) J Ind Eng Chem 12(1):149
4. Moon DJ, Ryu JW (2003) Catal Lett 89(3–4):207
5. Kang JS, Kim DH, Lee SD, Hong SI, Moon DJ (2007) Appl Catal A: Gen 332:153
6. Takehira K, Shishido T, Wang P, Kosaka T, Takaki K (2003) Phys Chem Chem Phys 5:3801
7. Choudary VR, Rajput AM, Prabhakar B (1993) J Catal 139:326
8. Moon DJ, Ryu JW, Lee SD, Lee BG, Ahn BS (2004) Appl Catal A: Gen 272:53
9. Kim DH, Kang JS, Lee YJ, Park NK, Kim YC, Hong SI, Moon DJ (2007) Catal Today 136(3–4):228
10. Acvi AK, Trimm DL, Aksoylu AE, Önsan Zİ (2004) Appl Catal A: Gen 258:235
11. Shishido T, Wang P, Kosaka T, Takehira K (2002) Chem Lett 31:752
12. Golunski S (1998) Platinum Met Rev 42:2
13. Trimm DL, Önsan Zİ (2001) Catal Rev-Sci Eng 43:31
14. Armor JN (1999) Appl Catal A: Gen 176:159
15. Bradford MCJ, Vannice MA (1991) Catal Rev Sci Eng 41:1
16. Dissanayake D, Rosynek MP, Kharas KCC, Lunsford JH (1991) J Catal 132:117
17. Trimm DL (1977) Catal Rev-Sci Eng 16:155
18. Kim JH, Suh DJ, Park TJ, Kim KL (2000) Appl Catal A: Gen 197:191
19. Tsyganok AI, Tsunoda T, Suzuki K, Hamakawa S, Takehira K, Hayakawa T (2003) J Catal 213:191
20. Moon DJ, Ryu JW, Kang DM, Lee BK, Ahn BS (2004) Stud Surf Sci Catal 153:193
21. Moon DJ, Ryu JW, Lee SD (2004) Stud Surf Sci Catal 153:149
22. Solymosi F, Tolmacsov P, Zakar TS (2005) J Catal 233:51
23. Takeguchi T, Kani Y, Ehuchi K, Aizwa M (2002) J Power Sources 112:588
24. Michael CJ, Vannice MA (1999) J Catal 183:69
25. Basile F, Basini L, D'Amore M, Fornasari G, Guarinoni A, Matteuzzi D, Del Piero G, Trifiro F, Vaccari A (1998) J Catal 173:247
26. Basini L, Guarinoni A, Aragano A (2000) J Catal 190:284
27. Bharadwaj SS, Schmidt LD (1995) Fuel Process Technol 42:109
28. Veser G, Schmidt LD (1996) AIChE J 42:177
29. Bharadwaj SS, Schmidt LD (1995) J Catal 155:403
30. Dietz AG, Schmidt LD (1995) Catal Lett 33:15
31. Witt PM, Schmidt LD (1996) J Catal 163:465
32. Shishido T, Sukenobu M, Morioka H, Kondo M, Wang Y, Takaki K, Takehira K (2002) Appl Catal A: Gen 223:35
33. Shishido T, Sukenobu M, Morioka H, Furukawa R, Shirahase H, Takehira K (2001) Catal Lett 73:21
34. Tsyganok AI, Suzuki K, Hamakawa S, Takehira K, Hayakawa T (2001) Catal Lett 77:75
35. Claridge JB, York APE, Brungs AJ, Marquez-Avarez C, Sloan J, Tsang SC, Green MLH (1998) J Catal 180:85
36. Minh NQ (1993) J Am Ceram Soc 76:563
37. Toebes ML, Bitter JH, van Dillen AJ, de Jong KP (2002) Catal Today 76:33
38. Baker RTK, Gadsby GR, Terry S (1975) Carbon 13:245
39. Park S, Craciun R, Vohs JM, Gorte RJ (1991) J Electrochem Soc 146:3603
40. Park S, Vohs J, Gorte R (2001) Nature (London) 404:265
41. McIntosh S, Vohs JM, Gorte RJ (2002) Electrochim Acta 47:3815
42. Zhao S, Gorte RJ (2003) Appl Catal A: Gen 248:9
43. Gorte RJ, Park S, Vohs JM, Wang C (2000) Adv Mater 12:1465
44. Kim H, Park S, Vohs J, Gorte R (2001) J Electrochem Soc 148:A693
45. Lu C, Worrell WL, Gorte RJ, Vohs JM (2003) J Electrochem Soc 150:A354
46. Lu C, Worrell WL, Vohs JM, Gorte RJ (2003) J Electrochem Soc 150(10):A1357
47. Lee BG, Kang JS, Kim DH, Lee SD, Moon DJ (2006) Stud Surf Sci Catal 159:617
48. Ryu JW, Park JM, Choi EH, Yoo KS, Nam SW, Hong SI, Moon DJ (2006) Stud Surf Sci Catal 159:613
49. Velu S, Swamy CS (1994) Appl Catal A: Gen 119:241
50. Corma A, Iborra S, Primo J, Rey F (1994) Appl Catal A: Gen 114:215
51. Katsuomi T, Tetsuya S, Peng W, Tokuhisa K, Ken T (2004) J Catal 221:43
52. Choudary BM, Madhi S, Chowdari N, Kantam ML, Sreedhar B (2002) J Am Chem Soc 124:14127
53. Tichit D, Coq B (2003) CAT TECH 7:206
54. Cavani F, Trifiro F, Vaccari A (1991) Catal Today 11:173
55. Hayakawa T, Suzuki S, Hamakawa S, Suzuki K, Shishido T, Takehira K (1999) Appl Catal A: Gen 183:273
56. Takehira K, Shishido T, Kondo M (2002) J Catal 207:307

57. Shiozaki R, Andersen AG, Hayakawa T, Hamakawa S, Suzuki K, Shimizu M, Takehira K (1997) J Chem Soc, Faraday Trans 93:3225
58. Moon DJ, Kim DH, Kang JS, Lee JS, Lee SD, Choi JS, Kim MJ (2008) In application to Korea Patent; (2008) PCT Patent
59. Recupero V, Pino L, Vita A, Cipiti F, Cordaro M, Laganà M (2005) Int J Hydrogen Energy 30(9):963
60. Velu S, Suzuki K, Gopinath CS (2002) J Phys Chem B 106:12746
61. Newson E, Truong TB (2003) Int J Hydrogen Energy 28:1379
62. Docter A, Lamm A (1999) J Power Sources 84:194
63. Bradford MCJ, Vannice MA (1999) Catal Rev 41:1
64. Li D, Atake I, Shishido T, Oumi Y, Sano T, Takehira K (2007) J Catal 250:299
65. Li D, Shishido T, Oumi Y, Sano T, Takehira K (2007) Appl Catal A: Gen 332:98
66. Nagaoka K, Jentys A, Lercher JA (2005) J Catal 229:185
67. Li B, Kado S, Mukainakano Y, Miyazawa T, Miyao T, Naito S, Okumura K, Kunimori K, Tomishige K (2007) J Catal 245:144
68. Moon DJ, Kim DH, Kang JS, Ryu JW, Lee BG, Yoon YS, Kwak BS (2005) Korea Patent 10-2005-00992; (2006) PCT Patent 2006-004047
69. Rostrup-Neilsen JR (2002) Catal Today 71:243
70. Douvartzides SL, Coutelieris FA (2003) J Power Sources 114:203
71. Erdohelyi A, Cserenyi J, Solymosi F (1993) J Catal 141:287
72. Qin D, Lapszewicz J (1994) Catal Today 21:551
73. Mark MF, Maier MF (1996) J Catal 164:122
74. Wang S, Lu GQ (1998) Energy Fuels 12:248
75. Xu Z, Li Y, Zhang J, Chang L, Zhou R, Duan Z (2001) Appl Catal A: Gen 210:45
76. Seo HJ, Yu EY (1997) J Ind Eng Chem 3:85
77. Roh HS, Jun KW, Park SE (2003) J Ind Eng Chem 9:261
78. Bradford MCJ, Vannice MA (1990) Catal Today 50:87
79. Tang SB, Qui FL (1995) Catal Today 24:253
80. Schulze K, Makowski W, Chyzy R, Dziembaj R, Geismar G (2001) Appl Clay Sci 18:59
81. Tsyganok AI, Suzuki K, Hamakawa S, Takehira K, Hayakawa T (2001) Chem Lett 30:24
82. Park SD, Vohs JM, Gorte RJ (2002) Nature 404:265
83. Ishihara T, Yamada T, Akbay T, Takita Y (1999) Chem Eng Sci 54:1535
84. Song C (2001) Chem Innov 31(1):21
85. Cho W, Baek Y, Moon SK, Kim YC (2002) Catal Today 74:207
86. Song C, Pan W (2004) Catal Today 98:463
87. Moon DJ, Kang DM, Ryu JW, Kim DH, Lee BK, Lee SD (2004) Fuel Cell Semin, San Antonio, TX
88. Moon DJ, Kang JS, Noh WS, Kim DH, Lee BG, Lee SD (2005) Korea Patent 10–0732729; (2007) US Patent 11-787555
89. Moon DJ, Kang JS, Shim JG, Noh WS, Gong KT, Lee HJ, Kim CS, Lee SD (2006) Fuel Cell Semin, Honolulu, Hawaii
90. Lee SH, Cho WC, Ju WS, Cho BH, Lee YC, Baek YS (2003) Catal Today 87:133
91. Moon DJ, Ryu JW, Kim TY, Lee SD, Lee BG (2003) Korea Patent 10-0569239
92. Moon DJ, Ryu JW, Park JM, Lee BG, Lee SD (2005) US Patent 2005-0089740 A1
93. Lim SS, Moon DJ, Kim JH, Kim YC, Park NK, Shin JS (2007) J Nanosci Nanotechnol 7(11):4013
94. Lee HR, Lee KY, Park NK, Shin JS, Moon DJ, Lee BG, Kim YC (2007) J Nanosci Nanotechnol 6(11):3396
95. Borowiecki T, Grzegorczyk W, Denis A, Golebiowski A (2002) Catal Lett 79:119
96. Kepinski L, Stasinska B, Borowiecki T (2000) Carbon 38:1845
97. Wang X, Gorte RJ (2002) Appl Catal A: Gen 224:209
98. Acvi AK, Trimm DL, Aksoylu AE, Önsan Zİ (2003) Catal Lett 88:17
99. Ahmed K, Gamman J, Föger K (2002) Solid State Ionics 152–153 (2002) 485
100. Suzuki T, Iwanami H-i, Iwamoto O, Kitahara T (2001) Int J Hydrogen Energy 26(9):935
101. Ghenciu AF (2002) Curr Opin Solid State Mater Sci 6:389
102. Joensen F, Rostrup-Nielsen JR (2002) J Power Sources 105:195
103. Mattos LV, Rodino E, Resasco DE, Possos FB, Noronha FB (2003) Fuel Process Technol 83:147
104. Roh HS, Jun KW, Park SE (2003) Appl Catal A: Gen 251:275
105. Laosiripojana N, Assabumrungrat S (2006) J Power Sources 158:1348
106. Ramirez-Cabrera E, Atkinson A, Chadwick D (2004) Appl Catal B 47:127
107. Fornasiero P, Balducci G, Monte RD, Kaspar J, Sergo V, Gubitosa G, Ferrero A, Graziani M (1996) J Catal 164:173
108. Miki T, Ogawa T, Haneda M, Kakuta N, Ueno A, Tateishi S, Matsuura S, Sato M (1990) J Phys Chem 94:6464
109. Imamura S, Shono M, Okamoto N, Hamada R, Ishida S (1996) Appl Catal A: Gen 142:279
110. Kacimi S, Barbier J Jr, Taha R, Duperz D (1993) Catal Lett 22:343
111. Pijolat M, Prin M, Soustelle M (1995) J Chem Soc, Faraday Trans 91:3941
112. Lim YS, Moon DJ, Park NK, Shin JS, Kim JH, Kim YC (2007) J Nanosci Nanotechnol 7(11):4009
113. Kim DH, Kang JS, Lee YJ, Hong SI, Moon DJ (2008) In: Communicated to 14th ICC Symposium, Seoul, Korea